Physics Letters B 806 (2020) 135464

Contents lists available at ScienceDirect

Physics Letters B

www.elsevier.com/locate/physletb

Impact of a thermal medium on D mesons and their chiral partners

Glòria Montaña [a], Àngels Ramos [a], Laura Tolós [b,c,d,e], Juan M. Torres-Rincon [b,*]

[a] Departament de Física Quàntica i Astrofísica and Institut de Ciències del Cosmos (ICCUB), Facultat de Física, Universitat de Barcelona, Martí i Franquès 1, 08028 Barcelona, Spain
[b] Institut für Theoretische Physik, Goethe Universität Frankfurt, Max von Laue Strasse 1, 60438 Frankfurt, Germany
[c] Frankfurt Institute for Advanced Studies, Ruth-Moufang-Str. 1, 60438 Frankfurt am Main, Germany
[d] Institute of Space Sciences (ICE, CSIC), Campus UAB, Carrer de Can Magrans, 08193, Barcelona, Spain
[e] Institut d'Estudis Espacials de Catalunya (IEEC), 08034 Barcelona, Spain

ARTICLE INFO

Article history:
Received 5 February 2020
Received in revised form 7 April 2020
Accepted 27 April 2020
Available online 5 May 2020
Editor: J.-P. Blaizot

Keywords:
Charmed mesons
Effective hadron theories
Finite-temperature QFT
Chiral symmetry
Heavy-quark symmetry
Chiral symmetry restoration

ABSTRACT

We study D and D_s mesons at finite temperature using an effective field theory based on chiral and heavy-quark spin-flavor symmetries within the imaginary-time formalism. Interactions with the light degrees of freedom are unitarized via a Bethe-Salpeter approach, and the D and D_s self-energies are calculated self-consistently. We generate dynamically the $D_0^*(2300)$ and $D_s(2317)$ states, and study their possible identification as the chiral partners of the D and D_s ground states, respectively. We show the evolution of their masses and decay widths as functions of temperature, and provide an analysis of the chiral-symmetry restoration in the heavy-flavor sector below the transition temperature. In particular, we analyse the very special case of the D-meson, for which the chiral partner is associated to the double-pole structure of the $D_0^*(2300)$.

1. Introduction

The idea that chiral partners become degenerate above the chiral restoration temperature T_χ [1,2] has motivated a large amount of works in which low-lying hadronic states of opposite parities have been studied in a thermal medium and their masses have been seen to merge at large temperatures $T > T_\chi$.

The canonical example resides in the light-meson sector, where the pseudoscalar isotriplet (π) and the scalar isoscalar (σ meson) acquire similar masses above T_χ. This system has been studied in the linear sigma model [3], the (P)NJL model [4–6], the quark-meson model [7] and others. On the other hand, vector and axial vector interactions, that have been studied in the (P)NJL model [8], and gauge linear-sigma model [9] for example, allow one to study the chiral symmetry restoration of the ρ and the a_1 states [2]. Opposite-parity diquarks also present such degeneracy in the (P)NJL model [10], whereas there exist also indications from lattice-QCD calculations of the chiral restoration of opposite-parity baryons [11,12].

In many of the theoretical models, the parity partners are fundamental degrees of freedom, e.g. π and σ in the linear sigma model [3], and interactions in a thermal/dense medium dress them producing in-medium mass modifications. In another set of models, e.g. the NJL and PNJL model, the parity partners (either $0^+/0^-$ or $1^+/1^-$) are not part of the degrees of freedom of the Lagrangian, but are instead generated from few-body dynamics, like those implemented by the Bethe-Salpeter equation for a quark-antiquark pair. In this case, masses and decay widths seem to converge in the chirally-restored phase [6].

All these models provide insights of the effects of chiral restoration, both below and above T_χ. However one should keep in mind that—although well-motivated by the QCD symmetries and dynamics—they are not usually the correct effective field theory (EFT) of QCD. In the light-meson sector, for instance, we know that the low-energy effective theory is chiral perturbation theory (ChPT) [13]. It can lead to model-independent results, also at finite temperatures. However, this approach is valid at low energies and temperatures, always below T_χ, and only timid indications of a chiral-symmetry restoration can be expected from it.

Even if limited to $T < T_\chi$, this chiral approach is quite interesting because a combined picture of the chiral partners comes into play. The negative parity partner π is a degree of freedom of the Lagrangian [13], whose vacuum mass is dressed by interactions with the whole set of (pseudo-) Goldstone bosons.

* Corresponding author.
E-mail addresses: gmontana@fqa.ub.edu (G. Montaña), ramos@fqa.ub.edu (À. Ramos), tolos@th.physik.uni-frankfurt.de (L. Tolós), torres-rincon@th.physik.uni-frankfurt.de (J.M. Torres-Rincon).

https://doi.org/10.1016/j.physletb.2020.135464

However, the positive parity partner (σ) is not part of the Lagrangian. In unitarized versions of ChPT [14,15] it can be associated to the $J^\pi = 0^+$ resonant state, appearing in the scalar isoscalar channel of the meson-meson scattering amplitude. This state—experimentally identified with the scalar $f_0(500)$ of the Particle Data Group [16]—can be generated at finite temperature as well [17,18]. This scenario, where one of the chiral companions is a degree of freedom of the theory and the other a dynamically-generated state, is the one we consider in this work.

In this letter we focus on light-heavy meson systems and look for the thermal effects on the D and D_s mesons properties, and of their chiral partners. For this goal, we extend previous results in a more complete and consistent approach using a hadronic EFT. The spirit is similar to Ref. [19] where a chiral $SU(4)$ effective Lagrangian at leading-order (LO) was used (see also [20] for a use of the same EFT). However, in the present work, we construct the interactions based on an effective Lagrangian based on $SU(3)$ chiral, and heavy-quark symmetries. This effective theory at next-to-leading-order (NLO) has been well studied in vacuum, and its low-energy parameters fixed by lattice-QCD fits [21–23]. The dynamics of the light-heavy meson systems is computed at finite temperature in the framework of the imaginary-time formalism (ITF), and we use unitarity and self-consistency as our guiding principles.

An important goal of this work is to study the spectroscopy of the heavy-light sector at finite temperature. This means that we are interested in accessing not only the masses and decay widths of the D and D_s mesons, but also of the states which appear dynamically upon unitarization, namely the $D_0^*(2300)$ and $D_{s0}^*(2317)$ states. It happens that these scalars, positive parity states could be associated with the chiral partners of the ground states. Therefore, we can describe the temperature dependence of their masses/widths in view of the possible restoration of chiral symmetry in heavy-light systems. Limited by low temperatures (below T_χ) we simply provide qualitative indications on how these states approach the chiral transition, not being able to describe what happens above it. Moreover we discuss a new peculiar picture of chiral companions as the $D_0^*(2300)$ is described by a double-pole structure. This is a new scenario for chiral symmetry restoration as one needs to study simultaneously the evolution with temperature of three states.

2. Effective Lagrangian and unitarized interactions at $T \neq 0$

At $T < T_\chi$ and assuming no baryon density, the thermal medium is essentially composed by the lighter mesons of the pseudoscalar meson octet. Their interactions at low energies are governed by ChPT, based on chiral power counting. The heavy $J^\pi = 0^-$ mesons, D and D_s, propagate through this medium behaving as Brownian particles, suffering from collisions with any of the light mesons. The interaction of the D-mesons with light particles is described by an effective Lagrangian based on both chiral and heavy-quark symmetries [24,25]. We use the version at NLO in the chiral expansion, similarly as in [21–23,26–29].

The LO Lagrangian reads

$$\begin{aligned}\mathcal{L}_{\rm LO} =& \langle \nabla^\mu D \nabla_\mu D^\dagger\rangle - m_D^2 \langle D D^\dagger\rangle \\ & - \langle \nabla^\mu D^{*\nu} \nabla_\mu D_\nu^{*\dagger}\rangle + m_D^2 \langle D^{*\nu} D_\nu^{*\dagger}\rangle \\ & + ig\langle D^{*\mu} u_\mu D^\dagger - D u^\mu D_\mu^{*\dagger}\rangle + \frac{g}{2m_D}\langle D_\mu^* u_\alpha \nabla_\beta D_\nu^{*\dagger} \\ & - \nabla_\beta D_\mu^* u_\alpha D_\nu^{*\dagger}\rangle \epsilon^{\mu\nu\alpha\beta}\,, \end{aligned} \tag{1}$$

where D denotes the antitriplet of 0^- D-mesons [$D = \begin{pmatrix} D^0 & D^+ & D_s^+ \end{pmatrix}$], and similarly for the vector 1^- states [$D_\mu^* = \begin{pmatrix} D^{*0} & D^{*+} & D_s^{*+} \end{pmatrix}_\mu$] (not used in this work)]. The light mesons are encoded into $u_\mu = i(u^\dagger \partial_\mu u - u \partial_\mu u^\dagger)$, where u is the unitary matrix of Goldstone bosons in the exponential representation. The bracket denotes the trace in flavor space and the connection of the covariant derivative $\nabla_\mu D^{(*)} = \partial_\mu D^{(*)} - D^{(*)}\Gamma^\mu$ reads $\Gamma_\mu = \frac{1}{2}(u^\dagger \partial_\mu u + u \partial_\mu u^\dagger)$.

The NLO Lagrangian is given by

$$\begin{aligned}\mathcal{L}_{\rm NLO} =& - h_0 \langle D D^\dagger\rangle \langle \chi_+\rangle + h_1 \langle D \chi_+ D^\dagger\rangle + h_2 \langle D D^\dagger\rangle \langle u^\mu u_\mu\rangle \\ & + h_3 \langle D u^\mu u_\mu D^\dagger\rangle + h_4 \langle \nabla_\mu D \nabla_\nu D^\dagger\rangle \langle u^\mu u^\nu\rangle \\ & + h_5 \langle \nabla_\mu D \{u^\mu, u^\nu\} \nabla_\nu D^\dagger\rangle + \tilde{h}_0 \langle D^{*\mu} D_\mu^{*\dagger}\rangle \langle \chi_+\rangle \\ & - \tilde{h}_1 \langle D^{*\mu} \chi_+ D_\mu^{*\dagger}\rangle - \tilde{h}_2 \langle D^{*\mu} D_\mu^{*\dagger}\rangle \langle u^\nu u_\nu\rangle \\ & - \tilde{h}_3 \langle D^{*\mu} u^\nu u_\nu D_\mu^{*\dagger}\rangle - \tilde{h}_4 \langle \nabla_\mu D^{*\alpha} \nabla_\nu D_\alpha^{*\dagger}\rangle \langle u^\mu u^\nu\rangle \\ & - \tilde{h}_5 \langle \nabla_\mu D^{*\alpha} \{u^\mu, u^\nu\} \nabla_\nu D_\alpha^{*\dagger}\rangle, \end{aligned} \tag{2}$$

where $\chi_+ = u^\dagger \chi u^\dagger + u \chi u$, with the quark mass matrix $\chi = \mathrm{diag}(m_\pi^2, m_\pi^2, 2m_K^2 - m_\pi^2)$.

For more details we recommend Refs. [26,27,22,28]. The low-energy constants (LECs, h_i with $i = 0, ..., 5$), have been revisited in this work in view of the recent study [23] based on lattice-QCD data.

The effective Lagrangian at LO+NLO provides the tree-level scattering amplitude for D and D_s mesons with light mesons,

$$\begin{aligned} V^{ij}(s,t,u) =& \frac{1}{f_\pi^2}\Big[\frac{C_{\rm LO}^{ij}}{4}(s-u) - 4C_0^{ij}h_0 + 2C_1^{ij}h_1 \\ & - 2C_{24}^{ij}\Big(2h_2(p_2\cdot p_4) + h_4\big((p_1\cdot p_2)(p_3\cdot p_4) \\ & + (p_1\cdot p_4)(p_2\cdot p_3)\big)\Big) \\ & + 2C_{35}^{ij}\Big(h_3(p_2\cdot p_4) + h_5\big((p_1\cdot p_2)(p_3\cdot p_4) \\ & + (p_1\cdot p_4)(p_2\cdot p_3)\big)\Big)\Big], \end{aligned} \tag{3}$$

where p_1 and p_2 (p_3 and p_4) are the momenta of the incoming (outgoing) mesons and $C_{\rm LO,0,1,24,35}$ are the isospin coefficients (see Table II in [22]). The i, j indices denote channels with given values of strangeness S and isospin I.

This amplitude is used as the kernel of an on-shell Bethe-Salpeter equation within a full coupled-channel basis, $T = V + VGT$, where T is the unitarized amplitude and G is the light-heavy two-body propagator, which contains medium effects (see Fig. 1a). In IFT, after a Matsubara summation and a continuation to real energies, the loop reads

$$\begin{aligned} & G_{D\Phi}(E, \vec{p}; T) \\ & = \int \frac{d^3q}{(2\pi)^3} \int d\omega \int d\omega' \frac{S_D(\omega, \vec{q}; T) S_\Phi(\omega', \vec{p} - \vec{q}; T)}{E - \omega - \omega' + i\varepsilon} \\ & \quad \times [1 + f(\omega, T) + f(\omega', T)], \end{aligned} \tag{4}$$

where D denotes the heavy meson and Φ the light meson. The vacuum contribution of the above loop function needs regularization. While a dimensionally regularized loop is used in [23], with subtraction constants fitted to lattice-QCD data, we employ a cutoff scheme, a procedure which simplifies the numerical treatment at finite temperature. The value of the UV cutoff is chosen such that the loop functions in both schemes agree at threshold. To simplify further, we eliminate the channel dependence by choosing a common value of 800 MeV, which is close to the obtained values for the different channels. We checked that our results for the scattering lengths at $T = 0$ are consistent with those obtained in [23].

At $T \neq 0$ the internal meson propagators receive medium corrections due to the light meson gas. In ChPT the pion mass and

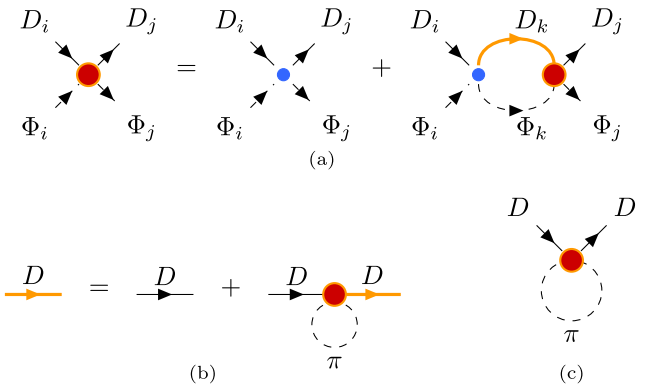

Fig. 1. (a) Bethe-Salpeter equation. The T-matrix is solved self-consistently with dressed internal heavy-meson propagator. (b) Dressed heavy-meson propagator. (c) Heavy-meson self-energy. The heavy meson is dressed by the unitarized interaction with pions (T-matrix, red dot).

decay constant do not appreciably change with temperature up to two-loops and even in unitary extensions of it [30,31]. In addition, the pion damping rate is very much suppressed at the temperatures explored in this paper, so we have decided to use the pion vacuum spectral function for all temperatures. For the D meson, we consider its medium modification through a self-consistent scheme consisting in using the T-matrix (Fig. 1a) to dress the propagator (Fig. 1b) with the D-meson self-energy (Fig. 1c) which reads,

$$\Pi_D(E,\vec{p};T) = \int \frac{d^3q}{(2\pi)^3} \int d\Omega \frac{E}{\omega_\pi} \frac{f(\Omega,T) - f(\omega_\pi,T)}{E^2 - (\omega_\pi - \Omega)^2 + i\varepsilon} \left(-\frac{1}{\pi}\right) \times \mathrm{Im}\, T_{D\pi}(\Omega, \vec{p}+\vec{q}; T)\,. \tag{5}$$

The D-meson spectral function to be used in the loop function is therefore,

$$S_D(\omega,\vec{q};T) = -\frac{1}{\pi}\mathrm{Im}\,\mathcal{D}_D(\omega,\vec{q};T) = -\frac{1}{\pi}\mathrm{Im}\left(\frac{1}{\omega^2 - \vec{q}^{\,2} - m_D^2 - \Pi_D(\omega,\vec{q};T)}\right). \tag{6}$$

This set of equations is solved iteratively until self-consistency is obtained.

3. Dynamically generated states at $T = 0$

Let us first discuss our findings at $T = 0$. In order to do so, we analytically continue the energy to the complex-energy plane and look for poles in the appropriate Riemann-sheet (RS) of the T-matrix, to find bound, resonant and virtual states. The pole position $\sqrt{s_R}$ provides the pole mass, $M_R = \mathrm{Re}\,\sqrt{s_R}$, and the width, $\Gamma_R/2 = \mathrm{Im}\,\sqrt{s_R}$. We also report the coupling, $|g_i|^{-2} = \partial T_{ii}^{-1}(s)/\partial s|_{s=s_R}$, of each pole to each of the channels i that the pole can couple.

In this letter we focus on the sectors $(S,I) = (0,\frac{1}{2})$—with three coupled channels, viz. $D\pi(2005.3)$, $D\eta(2415.1)$ and $D_s\bar{K}(2464.0)$—and $(S,I) = (1,0)$—with two coupled channels, $DK(2364.9)$ and $D_s\eta(2516.2)$, where the number in parentheses gives the corresponding threshold energy in MeV. We use the Fit-2B set of LECs used in [23], as it is the preferred one in that work and also the most similar to the one employed in [22]. Our results for the dynamically generated 0^+ partners are summarized in Table 1.

In the sector with $(S,I) = (0,\frac{1}{2})$ we find two poles in the complex energy plane. Both correspond to the experimental $D_0^*(2300)$ state [16]. This double-pole structure has been previously analyzed in [23,29]. The lower pole appears just above the first threshold in the $(-,+,+)$[1] RS of the T-matrix around 2080 MeV. The nature of the higher pole is a bit more complicated. We find it above the $D_s\bar{K}$ threshold as a pole in the $(-,-,+)$ RS, but for some values of the parameters of the model [23,29] the pole appears in the same sheet between the $D\eta$ and $D_s\bar{K}$ thresholds or below the $D\eta$ threshold[2], strongly coupled to the $D_s\bar{K}$ channel in all cases. The dependence on the parameters is described in detail in Ref. [23], but notice that it only brings slight modifications in the pole positions. Such an effect is not much relevant for our temperature-dependence study, as all parameters are fixed at $T = 0$.

Both poles have a considerable decay width so they are not close to the real energy axis. As we will see later, their reflection on the real axis will leave a peculiar structure, which one identifies with the experimental $D_0^*(2300)$. The lower pole couples mostly to $D\pi$, with reasonably large coupling to $D_s\bar{K}$, whereas the higher one couples to all the channels but with a larger coupling to $D_s\bar{K}$.

In the $(S,I) = (1,0)$ sector the situation is somewhat clearer. We find a single pole on the real axis, which we identify to the bound state $D_{s0}^*(2317)$. It has sizable couplings to both DK and $D_s\eta$, but it cannot decay to any of them as the phase space is closed at $T = 0$.

4. Spectral functions, masses, and widths at $T \neq 0$

We now present the results of our study at finite temperature. To begin with, we dedicate a few lines commenting on the limiting temperature in our approach, apart from the evident restriction $T < T_\chi$ already mentioned.

Light mesons composing the thermal bath are described by ChPT. According to its power counting the temperature is a soft scale contained in the expansion parameter $T/(Cf_\pi)$, with C a numerical factor. For example in the massless case one has $C = \sqrt{8}$ [32]. In the massive case, the first works established a limiting temperature of $T \simeq 150$ MeV [33], but in practice, this value should be reduced to $T \simeq 100$ MeV, when pions start having typical energies probing the ρ meson peak [30,31].

However the unitarized version of ChPT extends the validity of the theory to higher energies, therefore increasing the maximal temperature even above $T = 150$ MeV [17,30,34]. In particular, the application of the same unitarization method used in this work to the light sector [35] allows us to explain meson-meson scattering up to $\sqrt{s} = 1.2$ GeV (see also [36] for the same conclusion using an alternative unitarization method). On the other hand, at $T = 150$ MeV the mean thermal energy of a pion is $\langle E_\pi \rangle = 475$ MeV, and a pair of pions colliding head-on will have a typical $\sqrt{s} \simeq 950$ MeV, which can be described by the unitarized theory. For a $D - \pi$ head-on collision one has a typical $\sqrt{s} \simeq 2.6$ GeV, which is near the higher pole of the $D_0^*(2300)$ resonance, and therefore within the validity of our theory. While for kaons the typical thermal energies are higher and can exceed $\sqrt{s} = 1.2$ GeV, a generic collision will not occur head-on and the typical $\sqrt{s}$ decreases below the limit. In conclusion, we determine that $T = 150$ MeV should be a reasonable limiting temperature for our theory. Of course, one should take the results around this value with caution, because the fastest mesons might lie outside the validity of the theory and, in addition, the deconfined phase will start playing a role in the system.

The spectral functions of the D and D_s mesons follow the standard definition in terms of the retarded propagator, see Eq. (6).

[1] The notation indicates the RS of the loop function for each of the coupled channels (+ for first and − for second).

[2] We note that the $(-,-,+)$ RS is only connected to the real energy axis in the region between the $D\eta$ and the $D_s\bar{K}$ thresholds.

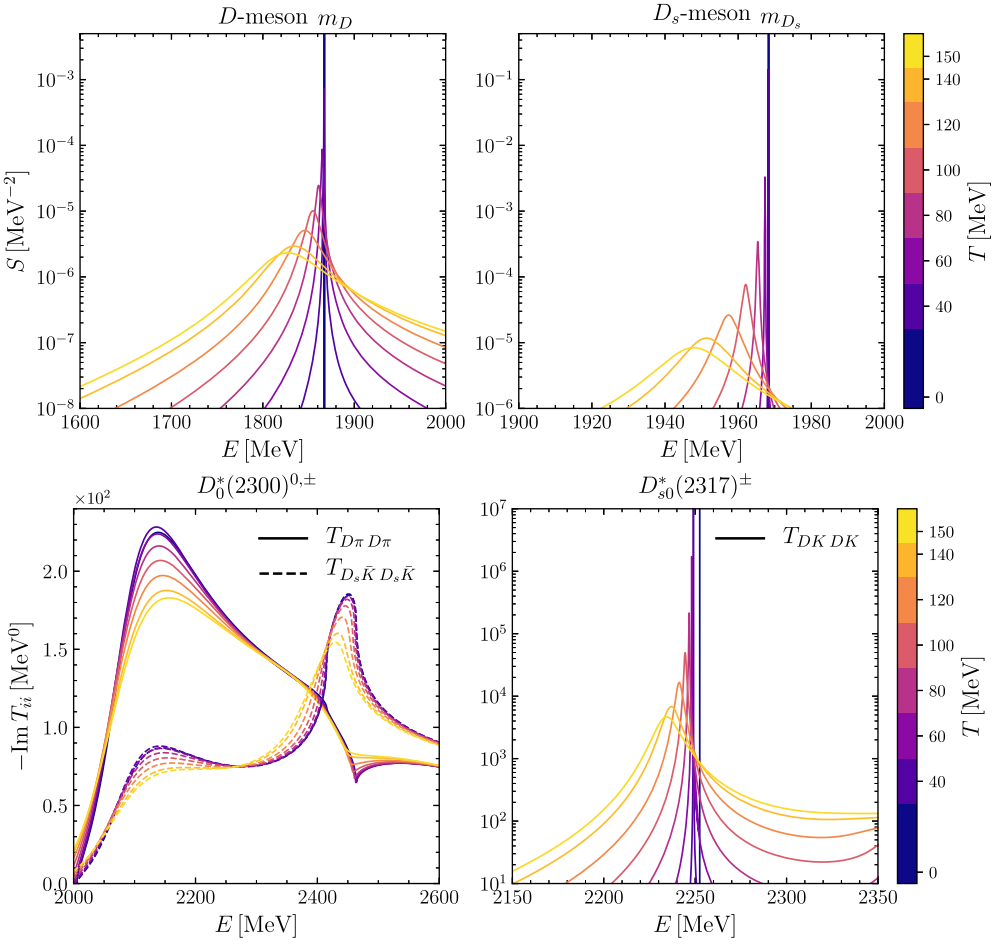

Fig. 2. Upper plots: spectral functions of the D- (left) and D_s-mesons (right) at different temperatures from 0 to 150 MeV. Lower plots: imaginary part of the $D\pi \to D\pi$ and $D_s\bar{K} \to D_s\bar{K}$ scattering amplitudes in the $(S, I) = (0, \frac{1}{2})$ sector (left) and the $DK \to DK$ amplitude for $(S, I) = (1, 0)$ (right) at the same values of the temperature.

They are shown on the top panels of Fig. 2 at zero trimomentum, as functions of the energy and for different temperatures (coloured lines). The mass shift and widening of both states with temperature is evident, being these effects stronger for the D-meson, whose mass decreases considerably with T. The properties of the dynamically generated states are directly obtained from the imaginary part of the amplitudes T_{ii} as a proxy for their spectral shape. It is presented in the bottom panels of Fig. 2, with i denoting the channel to which the state couples most, i.e. $D\pi$ ($D_s\bar{K}$) for the lower (higher) pole of the $D_0^*(2300)$ in the $(S, I) = (0, \frac{1}{2})$ sector, and DK for the pole of the $D_{s0}^*(2317)$ in the $(S, I) = (1, 0)$ sector. In the $S = 0$ case peculiar structures appear, which are produced by the interplay of the position of the resonance to some nearby channel thresholds. Still the evolution of the peak and width of the amplitudes with T is evident. For the $S = 1$ sector the situation is clearer, but one can observe that, in addition to the typical thermal widening, more strength is visible on the right-hand side tail producing a totally asymmetric distribution. The reason lies in the fact that the unitary DK threshold is lowered due to the decrease of the D mass and its widening with temperature, hence opening the phase space for decay into this channel at smaller energies.

Finally in Fig. 3 we represent the evolution of the masses and decay widths with temperature. Differently from the $T = 0$ case, the results of which we presented in Table 1, we find the determination of the poles in the complex energy plane unfeasible. Apart from complications tied to the analytic continuation of imaginary frequencies to the different RSs, a numerical search on the complex plane within self-consistency is computationally challenging.

Table 1
Poles and the corresponding couplings to the coupled channels of the physical $D_0^*(2300)$ (first two poles) and $D_{s0}^*(2317)$ (last pole).

	(S, I)	RS	M_R (MeV)	$\Gamma_R/2$ (MeV)	$\lvert g_i \rvert$ (GeV)
$D_0^*(2300)$	$(0, \frac{1}{2})$	$(-,+,+)$	2081.9	86.0	$\lvert g_{D\pi} \rvert = 8.9$ $\lvert g_{D\eta} \rvert = 0.4$ $\lvert g_{D_s\bar{K}} \rvert = 5.4$
		$(-,-,+)$	2521.2	121.7	$\lvert g_{D\pi} \rvert = 6.4$ $\lvert g_{D\eta} \rvert = 8.4$ $\lvert g_{D_s\bar{K}} \rvert = 14.0$
$D_{s0}^*(2317)$	$(1, 0)$	$(+,+)$	2252.5	0.0	$\lvert g_{DK} \rvert = 13.3$ $\lvert g_{D_s\eta} \rvert = 9.2$

Therefore, the mass and width will be obtained from the position and the half-width at half-maximum of the peak of the spectral functions in the real-energy axis. For the ground states, D and D_s, this method is totally acceptable as the quasi-particle approximation is entirely justified. However, for the dynamically generated states—at least in the $S = 0$ channel—this entails more problems because their poles are located far from the real axis and the width is not a well-defined concept. In view of these problems, we establish the following strategy, the details of which will be given in a subsequent publication,

- For the lower resonance in the $(S, I) = (0, \frac{1}{2})$ sector we assume a Breit-Wigner-Fano shape [37], which takes into account the interaction between the resonance and the back-

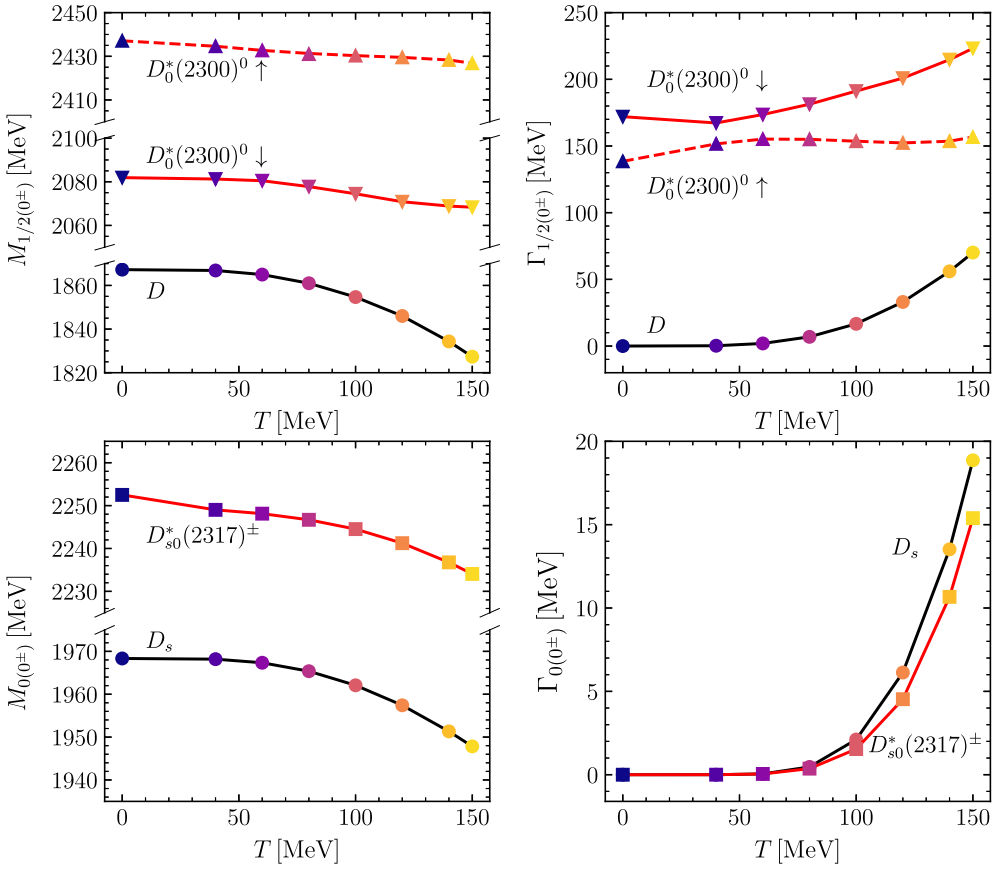

Fig. 3. Temperature evolution of the mass (left panels) and width (right panels) of the chiral partners in the $(S, I) = (0, \frac{1}{2})$ sector (upper panels) and in the $(S, I) = (1, 0)$ sector (lower panels). The ground-state 0^- partners are represented with circles and the dynamically generated 0^+ partners, the two poles of the $D_0^*(2300)$ and the $D_{s0}^*(2317)$ pole, with upward/downward triangles and squares, respectively.

ground corresponding to the higher resonance. The mass and width of the fit at $T = 0$ are in very good agreement with the values of the pole mass and the width in Table 1.

- For the higher resonance in the $(S, I) = (0, \frac{1}{2})$ sector we subtract the background contribution of the lower resonance and then fit a Flatté-type distribution that describes the shape of resonances in the proximity of a threshold [38], extended here to the three coupled-channel case. We note that this fitting procedure is very sensitive to fitting details. We present here the results for the masses and widths with fitting parameters constrained by the behaviour of the T-matrix around that resonance as seen in the lower left panel of Fig. 2. We defer a thorough study of the uncertainties tied to the fitting procedure to a subsequent publication.
- For the resonance in the $(S, I) = (1, 0)$ sector we again fit a Breit-Wigner-Fano distribution, although a simple fit with a Breit-Wigner gives the same results for $T < 120$ MeV.

From the results in Fig. 3 and in comparison with previous works, we list the following observations:

1. The ground state D mass has a sizable decrease of $\Delta m_D \sim 40$ MeV at the highest temperature $T = 150$ MeV. This reduction is consistent, albeit twice larger, with that observed in [39], where a more phenomenological approach is used to compute the D-meson propagator. Our reduction, on the other hand, is smaller than the one reported in Ref. [40], that uses non-unitarized ChPT. However, in the $SU(4)$ effective approach of [19] no significant modification is reported. In our present work the two poles of the $D_0^*(2300)$ have a more stable trend. They slightly move downwards, moderately distancing from each other. Therefore, in this sector we cannot conclude that masses of opposite parity states become degenerate close to T_χ, although the temperatures studied might be still low for the chiral symmetry restoration. In [41] a large reduction in the mass of the positive-parity D meson partner, of around 150 MeV, is found at $T = 150$ MeV, but using a constant D mass as an input of the sum-rule analysis. An even larger reduction of close to 200 MeV is seen in the results of [40].
2. The width of all states in the non-strange sector increases with temperature. The ground state shows a width of around ~ 70 MeV at $T = 150$ MeV, consistent with [19] and the estimates of Refs. [39,42]. The widths of the two poles of the $D_0^*(2300)$ obtained from the fits increase moderately with temperature with respect to their vacuum value.
3. In the strangeness sector we observe a clearer picture. The parity partners seem to decrease their mass with temperature, in a similar amount for both states, reaching a reduction of ~ 20 MeV for the 0^- state and ~ 19 MeV for the 0^+ state at $T = 150$ MeV. Consequently, they are still far from chiral degeneracy. These behaviours seem to be compatible with the low temperature trends seen in the linear-sigma model calculation of [40].
4. The decay widths of both strange partners increase from zero at similar rates. The width of the $D_{s0}^*(2317)$ is comparable to that acquired by the D_s ground state at $T = 150$ MeV. We note that, whereas the width of the latter is only due to medium effects, the $D_{s0}^*(2317)$ also contains the additional contribution of the decay into DK states due to the reduction of the mass

and the widening of the D-meson. We are not aware of any previous result to compare to in this sector.

Apart from the above comparisons with previous models, unfortunately there is no solid data from first principles to compare to. However, in spite of the limitations in obtaining reliable information from finite temperature lattice QCD simulations tied to the difficulties in extracting the spectral function from the lattice correlators, we can still aim at a qualitative comparison. We note that a recent lattice-QCD calculation [43] presents the spectral functions of D and D_s channels at different temperatures. The analysis in that paper concludes that no medium modification with respect to the D and D_s ground states is seen up to T_χ, where $T_\chi \simeq 185$ MeV in that work. Given the precision of the lattice-QCD data this might be well in agreement with our findings here, as our D (D_s) mass shift is only 2% (1%) of the mass itself. As a pion mass of $m_\pi \sim 380$ MeV is used in [43], it would be interesting to re-address our calculation with a heavier pion mass and analyze the effects on the charm meson properties for temperatures $T < T_\chi$.

5. Conclusion

In this letter we report our findings on the properties of heavy-light mesons at finite temperatures. Using a thermal effective field theory based on chiral and heavy-quark symmetries at NLO, and on the basis of unitarized scattering amplitudes and self-consistency, we have obtained the temperature dependence of the spectral functions of the chiral partners, D and $D_0^*(2300)$, as well as those of the D_s and $D_s^*(2317)$ mesons.

From these spectral functions, we have extracted the dependence of the masses and widths of the mesons with temperature. In the $(S, I) = (0, \frac{1}{2})$ and $(S, I) = (1, 0)$ sectors we do not observe a clear tendency to chiral degeneracy. However, we are limited by the low-temperature application of the hadron effective theory and, from the results of effective models in the light sector [5,44], such degeneracy might occur at higher temperatures, $T > T_\chi$.

One of our main results is that the chiral partner of the D meson, the $D_0^*(2300)$, has a double-pole structure in the complex-energy plane, and it is unclear at this point how the chiral symmetry restoration should be realized. Will both poles merge into a single one before becoming degenerate with the ground state? Or will only one pole survive and become degenerate with the ground state at $T > T_\chi$, while the other follows a different path?

Finally, we should mention that these results are important for a realistic analysis of heavy-ion collisions using appropriately medium-modified properties and/or heavy-flavor transport coefficients [28,45–48]. This is mandatory to understand the mechanisms of charm production and properly characterise the deconfined and hadronic phases. We plan to address studies in that direction in the future.

6. Acknowledgements

J.M.T.-R. acknowledges the hospitality of the Institut de Ciències de l'Espai (CSIC) and the Universitat de Barcelona, where part of this work was carried out. He thanks discussion with Á. Gómez-Nicola and J.A. Oller on the subject.

G.M. and A.R. acknowledge support from the Spanish Ministerio de Economía y Competitividad (MINECO) under the project MDM-2014-0369 of ICCUB (Unidad de Excelencia "María de Maeztu"), and, with additional European FEDER funds, under the contract FIS2017-87534-P. G.M. also acknowledges support from the FPU17/04910 Doctoral Grant from MINECO. L.T. acknowledges support from the FPA2016-81114-P Grant from Ministerio de Ciencia, Innovación y Universidades, Heisenberg Programme of the Deutsche Forschungsgemeinschaft (DFG, German research Foundation) under the Project No. 383452331 and THOR COST Action CA15213. L.T. and J.M.T.-R. acknowledge support from the DFG through projects no. 411563442 (Hot Heavy Mesons) and no. 315477589 - TRR 211 (Strong-interaction matter under extreme conditions).

Declaration of competing interest

The authors declare that they have no known competing financial interests or personal relationships that could have appeared to influence the work reported in this paper.

References

[1] T. Hatsuda, T. Kunihiro, Fluctuation effects in hot quark matter: precursors of chiral transition at finite temperature, Phys. Rev. Lett. 55 (1985) 158–161.
[2] R. Rapp, J. Wambach, Chiral symmetry restoration and dileptons in relativistic heavy ion collisions, Adv. Nucl. Phys. 25 (2000) 1.
[3] A. Bochkarev, J.I. Kapusta, Chiral symmetry at finite temperature: linear versus nonlinear sigma models, Phys. Rev. D 54 (1996) 4066–4079.
[4] S.P. Klevansky, The Nambu-Jona-Lasinio model of quantum chromodynamics, Rev. Mod. Phys. 64 (1992) 649–708.
[5] W. Florkowski, B.L. Friman, Screening of the meson fields in the Nambu-Jona-Lasinio model, Acta Phys. Pol. B 25 (1994) 49–71.
[6] H. Hansen, W.M. Alberico, A. Beraudo, A. Molinari, M. Nardi, C. Ratti, Mesonic correlation functions at finite temperature and density in the Nambu-Jona-Lasinio model with a Polyakov loop, Phys. Rev. D 75 (2007) 065004.
[7] R.-A. Tripolt, N. Strodthoff, L. von Smekal, J. Wambach, Spectral functions for the quark-meson model phase diagram from the functional renormalization group, Phys. Rev. D 89 (2014) 034010.
[8] B. Sintes, Etude des baryons avec le modèle de Nambu et Jona-Lasinio, Ph.D. thesis, SUBATECH, Nantes, 2014, https://tel.archives-ouvertes.fr/tel-01180392.
[9] R.D. Pisarski, Where does the rho go? Chirally symmetric vector mesons in the quark-gluon plasma, Phys. Rev. D 52 (1995) R3773–R3776.
[10] J.M. Torres-Rincon, B. Sintes, J. Aichelin, Flavor dependence of baryon melting temperature in effective models of QCD, Phys. Rev. C 91 (2015) 065206.
[11] G. Aarts, C. Allton, D. De Boni, S. Hands, B. Jäger, C. Praki, J.-I. Skullerud, Light baryons below and above the deconfinement transition: medium effects and parity doubling, J. High Energy Phys. 06 (2017) 034.
[12] G. Aarts, C. Allton, D. De Boni, B. Jäger, Hyperons in thermal QCD: a lattice view, Phys. Rev. D 99 (2019) 074503.
[13] J. Gasser, H. Leutwyler, Chiral perturbation theory to one loop, Ann. Phys. 158 (1984) 142.
[14] A. Dobado, M.J. Herrero, T.N. Truong, Unitarized chiral perturbation theory for elastic pion-pion scattering, Phys. Lett. B 235 (1990) 134–140.
[15] A. Dobado, J.R. Pelaez, The inverse amplitude method in chiral perturbation theory, Phys. Rev. D 56 (1997) 3057–3073.
[16] M. Tanabashi, et al., Particle Data Group, Rev. Part. Phys., Phys. Rev. D 98 (2018) 030001.
[17] A. Dobado, A. Gomez Nicola, F.J. Llanes-Estrada, J.R. Pelaez, Thermal rho and sigma mesons from chiral symmetry and unitarity, Phys. Rev. C 66 (2002) 055201.
[18] R. Rapp, J. Wambach, Thermal properties of a hot pion gas beyond the quasiparticle approximation, Phys. Lett. B 351 (1995) 50–55.
[19] M. Cleven, V.K. Magas, A. Ramos, Properties of open and hidden charm mesons in light quark matter, Phys. Rev. C 96 (2017) 045201.
[20] A. Mishra, E.L. Bratkovskaya, J. Schaffner-Bielich, S. Schramm, H. Stoecker, Mass modification of D meson in hot hadronic matter, Phys. Rev. C 69 (2004) 015202.
[21] F.-K. Guo, C. Hanhart, U.-G. Meissner, Interactions between heavy mesons and Goldstone bosons from chiral dynamics, Eur. Phys. J. A 40 (2009) 171–179.
[22] L. Liu, K. Orginos, F.-K. Guo, C. Hanhart, U.-G. Meissner, Interactions of charmed mesons with light pseudoscalar mesons from lattice QCD and implications on the nature of the $D_{s0}^*(2317)$, Phys. Rev. D 87 (2013) 014508.
[23] Z.-H. Guo, L. Liu, U.-G. Meißner, J.A. Oller, A. Rusetsky, Towards a precise determination of the scattering amplitudes of the charmed and light-flavor pseudoscalar mesons, Eur. Phys. J. C 79 (2019) 13.
[24] E.E. Kolomeitsev, M.F.M. Lutz, On heavy light meson resonances and chiral symmetry, Phys. Lett. B 582 (2004) 39–48.
[25] M.F.M. Lutz, M. Soyeur, Radiative and isospin-violating decays of D(s)-mesons in the hadrogenesis conjecture, Nucl. Phys. A 813 (2008) 14–95.
[26] L.S. Geng, N. Kaiser, J. Martin-Camalich, W. Weise, Low-energy interactions of Nambu-Goldstone bosons with D mesons in covariant chiral perturbation theory, Phys. Rev. D 82 (2010) 054022.
[27] L.M. Abreu, D. Cabrera, F.J. Llanes-Estrada, J.M. Torres-Rincon, Charm diffusion in a pion gas implementing unitarity, chiral and heavy quark symmetries, Ann. Phys. 326 (2011) 2737–2772.

[28] L. Tolos, J.M. Torres-Rincon, D-meson propagation in hot dense matter, Phys. Rev. D 88 (2013) 074019.
[29] M. Albaladejo, P. Fernandez-Soler, F.-K. Guo, J. Nieves, Two-pole structure of the $D_0^*(2400)$, Phys. Lett. B 767 (2017) 465–469.
[30] A. Schenk, Pion propagation at finite temperature, Phys. Rev. D 47 (1993) 5138–5155.
[31] D. Toublan, Pion dynamics at finite temperature, Phys. Rev. D 56 (1997) 5629–5645.
[32] J. Gasser, H. Leutwyler, Light quarks at low temperatures, Phys. Lett. B 184 (1987) 83–88.
[33] J. Goity, H. Leutwyler, On the mean free path of pions in hot matter, Phys. Lett. B 228 (1989) 517–522.
[34] A. Gomez Nicola, F.J. Llanes-Estrada, J. Pelaez, Finite temperature pion scattering to one loop in chiral perturbation theory, Phys. Lett. B 550 (2002) 55–64.
[35] J.A. Oller, E. Oset, J.R. Pelaez, Nonperturbative approach to effective chiral Lagrangians and meson interactions, Phys. Rev. Lett. 80 (1998) 3452–3455.
[36] A. Gomez Nicola, J. Pelaez, Meson-meson scattering within one loop chiral perturbation theory and its unitarization, Phys. Rev. D 65 (2002) 054009.
[37] U. Fano, Effects of configuration interaction on intensities and phase shifts, Phys. Rev. 124 (1961) 1866–1878.
[38] S.M. Flatte, Coupled-channel analysis of the pi eta and K anti-K systems near K anti-K threshold, Phys. Lett. B 63 (1976) 224–227.
[39] C. Fuchs, B.V. Martemyanov, A. Faessler, M.I. Krivoruchenko, D-mesons and charmonium states in hot pion matter, Phys. Rev. C 73 (2006) 035204.
[40] C. Sasaki, Fate of charmed mesons near chiral symmetry restoration in hot matter, Phys. Rev. D 90 (2014) 114007.
[41] T. Buchheim, T. Hilger, B. Kämpfer, S. Leupold, Chiral-partner D mesons in a heat bath within QCD sum rules, J. Phys. G 45 (2018) 085104.
[42] M. He, R.J. Fries, R. Rapp, Thermal relaxation of charm in hadronic matter, Phys. Lett. B 701 (2011) 445–450.
[43] A. Kelly, A. Rothkopf, J.-I. Skullerud, Bayesian study of relativistic open and hidden charm in anisotropic lattice QCD, Phys. Rev. D 97 (2018) 114509.
[44] T. Hatsuda, T. Kunihiro, QCD phenomenology based on a chiral effective Lagrangian, Phys. Rep. 247 (1994) 221–367.
[45] V. Ozvenchuk, J.M. Torres-Rincon, P.B. Gossiaux, L. Tolos, J. Aichelin, *D*-meson propagation in hadronic matter and consequences for heavy-flavor observables in ultrarelativistic heavy-ion collisions, Phys. Rev. C 90 (2014) 054909.
[46] T. Song, H. Berrehrah, D. Cabrera, J.M. Torres-Rincon, L. Tolos, W. Cassing, E. Bratkovskaya, Tomography of the quark-gluon-plasma by charm quarks, Phys. Rev. C 92 (2015) 014910.
[47] L. Tolos, J.M. Torres-Rincon, S.K. Das, Transport coefficients of heavy baryons, Phys. Rev. D 94 (2016) 034018.
[48] S.K. Das, J.M. Torres-Rincon, L. Tolos, V. Minissale, F. Scardina, V. Greco, Propagation of heavy baryons in heavy-ion collisions, Phys. Rev. D 94 (2016) 114039.